Journal of Molecular Liquids 322 (2021) 114761

Contents lists available at ScienceDirect

Journal of Molecular Liquids

journal homepage: www.elsevier.com/locate/molliq

Adsorption efficiency of sulfonated poly (ether ether ketone) (sPEEK) as a novel low-cost polymeric adsorbent for cationic organic dyes removal from aqueous solution

Jülide Hızal *, Nergiz Kanmaz, Mesut Yılmazoğlu

Yalova University, Faculty of Engineering, Department of Chemical Engineering, 77100 Yalova, Turkey

ARTICLE INFO

Article history:
Received 9 August 2020
Received in revised form 30 October 2020
Accepted 10 November 2020
Available online 05 December 2020

Keywords:
Methylene blue
Basic violet 16
Sulfonated poly (ether ether ketone)
Adsorption
Characterization

ABSTRACT

The aim of this study is to investigate the methylene blue (MB) and basic violet 16 (BV16) as cationic organic dyes adsorption on sulfonated poly(ether ether ketone) (sPEEK) in aqueous solution. sPEEK was synthesized, then characterized by FTIR, SEM, TGA, BET/N_2 surface area analysis, particle size and zeta potential measurements. Batch experiments were performed to analyze the effects of key parameters such as contact time, initial concentration and pH on MB and BV16 adsorptions. Additionally, temperature effect was investigated for MB adsorption. Kinetic data revealed that cationic dyes adsorptions were well-fitted by pseudo-second order kinetic model. The required times to achieve equilibrium were determined as 40 and 20 min for MB and BV16, respectively. The adsorptions showed Langmuirian character, and the maximum adsorption capacities were found to be 98.04 mg/g (0.29 mmol/g) for MB, and 181.8 mg/g (0.50 mmol/g) for BV16. The thermodynamic data showed that the MB adsorption was an endothermic process occuring spontaneously at room temperature. Desorption and recycling experiments showed that the adsorption efficiency decreased from 99.6% to 99.2% after the fifth cycle, pointing out sPEEK reusability for MB removal. Low desorption percentage of BV16 loaded sPEEK shows that sPEEK may be used for immobilizing of BV16.

1. Introduction

Following the resent developments in the textile industry significant amounts of organic dye wastes contaminates surface water every year. Azo type dyes contain one or more azo bonds (—N=N—) in association with the structure. Azo dyes are widely used to color textiles, paper, pigments and plastics, and nearly 30–70% of used azo dyes are hydrolyzed and mixes with the wastewater [1]. Therefore very large amounts of colored wastes discharge into the hydrosphere [2]. The removal of organic azo dyes is of great importance due to their carcinogenic and teratogenic effects on living organisms. Azo dye wastewater remediation is quite demanding since azo dyes are highly non-biodegradable and demonstrate high thermal, optical and physicochemical stability [3].

Methylene blue (MB), a widely used cationic dye which has versatile uses in several industries, is considered as a highly toxic, carcinogenic, and mutagenic water pollutant [4]. MB may cause eye and skin irritation, shortness of breath, rapid heartbeat, nausea and mental confusion. The presence of MB in the aquatic environments impedes the penetration of sunlight, diminishes photosynthesis and hence damages the aquatic ecosystems [5]. Consequently, it is essential to develop effective methods to remove MB from wastewater. Various methods such as flocculation precipitation [6], electrolysis [7], photocatalysis [8,9], ion exchange [10,11] and adsorption [12–17] have been used to remove dye-based pollutants from wastewaters. However these methods other than adsorption are quite complex, poor in decolorization efficiency and also can generate easy-to-produce by-products. Adsorption is an effecient and the most comprehensive technique, which has been used for the removal of azo dyes from industrial wastewaters, because of its ability to remove dyes at any concentration, easy to design and to be low-cost application [12,13]. Wang et al. magnetically separated MB from wastewater by using Fe_3O_4 nanoparticles embedded polyphosphazene (PZS) nanotube as adsorbent, and the results were compared with the results obtained from gallic acid modified Fe_3O_4 nanoparticles-polyphosphazene (PZS) nanotube. The results showed that the modifying with gallic acid enhanced the maximum adsorption capacity, and reduced the time required to equilibrium [14]. Prajapati et al. were used the waste coconut shell for the preparation of nanoporous activated carbon (NPAC) synthesized CuO nanoparticles were loaded on the NPAC (CuO-NPAC) and the prepared nanocomposites were compared the adsorption capacities for removal of MB from water. The maximum adsorption capacity of CuO-NPAC for MB is higher than activated carbon, nanoparticle and nanocomposites [17]. Yılmaz

* Corresponding author at: Yalova University, Faculty of Engineering, Department of Chemical Engineering, 77100 Yalova, Turkey.
E-mail address: hizalyucesoy@yalova.edu.tr (J. Hızal).

https://doi.org/10.1016/j.molliq.2020.114761
0167-7322/

et al. studied on pumice coated with poly(N-[Tris(hydroxymethyl) methyl]acrylamide) for MB adsorption. The authors stated that the removal efficiency was 98.68%, and the maximum adsorption capacity was 68.998 mg/g [16].

Basic violet 16 (BV16) is a highly soluble, non-volatile cationic dye with experimentally proven carcinogenic effects and toxicity against living organisms. Although widely used in the textile industry, it is a good quality water tracer fluorescent [18,19]. As with MB cationic dye removal, BV16 cationic dye can be also removed by expensive systems with high energy requirement such as ozonation, chemical oxidation, microbial degradation and membrane separation processes [18]. Recently, in several study it was preferred to perform BV16 dye removal by adsorption processes, with advantages such as low cost, simplicity of design and high removal efficiency. Shirazi et al. studied adsorption efficiencies of clay based adsorbents and charred dolomite on BV16. They showed that multi-adsorbent system of bentonite and charred dolomite removed both the anionic and cationic dyes effectively and simultaneously with removal efficiency of >70% [20]. Arami et al. Prepared and studied a novel biosorbent (*Canola* hull) for Basic Blue 41, Basic Red 46 and Basic Violet 16 as textile cationic dyes. Kinetic experiments of dyes followed pseudo-second order kinetics and the thermodynamic studies showed that the dye adsorption onto biosorbent is spontaneous and endothermic [21]. Adsorbents prepared from avocado kernel seeds were prepared and studied for basic violet 16 and basic blue by González et al. [22]. The results showed an enhanced adsorption capacity of the non-carbonized adsorbent upon cationic dyes in comparison with carbonized samples, due to the active surface acidic groups. Vosoughi et al. Studied the optimization of the removal of BV16 by the response surface methodology. They indicated that the desirable removal was obtained with the efficiency of 95.03% by a magnetite graphene oxide nanocomposites (Fe_3O_4@GO) under the dye concentration of 62.5 mgL^{-1} and the reaction time of 60 min [23].

sPEEK emerges as an inexpensive polymeric material that is mainly used as a fuel cell membrane as an alternative to widely used-conventional proton exchange membrane (Nafion, DuPont). Mehri et al. studied the performance of an electrocatalytic membrane reactor consisting Nafion and sPEEK as two different PEMs in desulfurization of a model diesel fuel containing thiophene and/or benzothiophene. They reported desulfurization efficiency of 85% at 20 mA/cm^2 and 75% at 30 mA/cm^2 was obtained for thiophene using Nafion and sPEEK, respectively. Similarly, enzothiophene desulfurization efficiencies of Nafion and sPEEK were about 70% and 65%, respectively [24]. Structurally modified Nafion-based adsorbents have been used in many water treatment studies. Nasef et al. studied the removal of heavy metal ions *e.g.* Ni(II), Co(II), Pb(II), Cu(II) and Ag(I) from aqueous solutions using Nafion-117 membrane under various treatment parameters including contact time, initial concentration, pH and temperature of the sorption medium [25]. Wang et al. prepared Nafion coated TiO_2(Nf/TiO_2) films for modifying the surface charge of TiO_2. They examined the effects of solution pH on the photoelectrochemical properties of TiO_2 photoelectrode and the adsorption behavior and photocatalytic reactions of Reactive Red 22 and Basic Red 2 in aqueous solution using various photocatalyst films (TiO_2 and Nafion-coated TiO_2, Nf/TiO_2) in a planar reactor [26].

In this study, sPEEK as an effective and low-cost adsorbent was synthesized and characterized. Because PEEK does not have any functional groups to interact with cationic dye, and assuming the sulfonated form of PEEK would enable to interact with positive charge of cationic dye, sPEEK was choosen as adsorbent. It was used for removal of cationic organic dyes MB and BV16 from aqueous solutions. The effects of contact time, solution pH, initial dye concentration on adsorption were investigated using batch experiments. The thermodynamic parameters were determined for MB adsorption. The dyes adsorptions were evaluated considering various isotherm models having different assumptions. The isotherm models were also treated on experimental data obtained from MB adsorption on PEEK. Additionally, the regeneration and reusability of sPEEK were also inspected using multicycle adsorption/desorption tests.

2. Materials and methods

2.1. Materials

Poly(ether ether ketone) (PEEK) was obtained from Röchling Sustaplast SE & Co. Sulfuric acid (98%), hydrochloric acid (37%, fuming), nitric acid (65%), sodium hydroxide and ethanol (96%) were purchased from Merck. Methylene blue ($C_{16}H_{18}ClN_3S$, purity>99.5%) was obtained from Sigma-Aldrich, and Basic Violet 16 was obtained from Strong Dyes (purity>99.5%).

2.2. Sulfonation of PEEK

5.0 g (Mettler Toledo XS105DU) PEEK was dissolved in 50 mL of concentrated sulfuric acid at 80 °C by magnetic stirring (WISD MSH-20D). At the end of a two-hour sulfonation reaction, a red viscous solution was obtained. The solution was rapidly dropped into 1 L of pre-cooled distilled water. Spherical sPEEK particles were washed with distilled water until pH 5–6. The prepared sPEEK beads were dried (BINDER ED115) at 65 °C for 48 h.

2.3. Determination of ion exchange capacity (IEC) and sulfonation degree (SD) of sPEEK

0.2 g sPEEK was stirred with saturated NaCl solution at 50 °C for 48 h. In principle of this process is carried out by the displacement of H^+ and Na^+ ions with sulfonic acid groups. After stirring, the sorbent was filtered, dried and titrated with 0.1 N NaOH. The IEC value was calculated by using the following equation:

$$IEC = \frac{V_{NaOH} \times N_{NaOH}}{W_p} \quad (1)$$

where V_{NaOH} and N_{NaOH} are the volume (mL) and normality (N) of the titrant, respectively, W_p is the amount (g) of dry adsorbent after saturation with NaCl solution.

The sulfonation degree of sPEEK was calculated by the following equation using IEC value:

$$SD\% = \frac{M_o \times IEC}{1000 - (M_1 \times IEC)} \times 100 \quad (2)$$

where M_o is repetitive unit mass of poly (ether ether ketone) which is equal to 288 g/mol, M_1 is the molar mass of SO_3Na which is equal to 103 g/mol.

2.4. Characterization of sPEEK

Following the synthesis, characterization of the sorbent was performed by using several methods. The morphology of sPEEK and dye loaded sPEEK samples have been studied using a JEOLTM JCM-6000 Plus NeoScope scanning electron microscope (SEM) operated at 15 kV. Fourier transform infra-red (FTIR) (Perkin Elmer, Spectrum 100) was used to analyze the functional groups of loaded and unloaded adsorbents by scanning in the wavelength range from 500 to 4000 cm^{-1}. The thermal behavior was investigated by thermogravimetric analysis (TGA) (SEIKO TG/DTA 6300) at a heating rate of 10 °C/min. Further surface investigations were performed using B.E.T./N_2 (Quantachrome Autosorb 1) surface area analysis, particle size and zeta potential measurements (Mastersizer 2000 hydro 2000 mu).

2.5. Batch experiments

The kinetic properties of MB and BV16 adsorption were investigated by measuring the organic dyes concentration depending the contact time. 10 mL of 100 mg/L dye solutions were contacted with 0.05 g sPEEK samples for 5 to 60 min for MB and 5 to 30 min for BV16 at room temperature and at 25 rpm on a rotator (Wisemix RT-10) while maintaining the solid/liquid ratio at 5.0 g/L. The heterogeneous mixture was filtrated through Whatman quantitative filter paper blue ribbon. The equilibrium studies were performed by shaking 0.05 g of sPEEK with 10 mL dye solutions having different initial concentration (100–1500 mg/L) for 40 and 20 min for MB and BV16, respectively. This procedure was repeated at 25 °C and 40 °C for MB adsorption. In order to determine the effect of pH on dyes adsorption, 0.05 g sPEEK was shaked with 10 mL of dye solutions whose initial concentrations were 250 mg/L for MB and 700 mg/L for BV16. The pHs of suspensions were adjusted between 1 and 12 by using 1 M NaOH and 20% HCl solutions. Additionally, MB adsorption on PEEK was performed in a similar way with that on sPEEK to exhibit contribution of sulfonation. The initial concentration of MB was changed between 100 and 1000 mg/L.

The equilibrium dye concentrations were measured by UV–Vis spectrophotometer (T80+ UV/VIS Spectrometer) at 665 and 546 nm for MB and BV16, respectively. The schematic diagram of adsorption process was introduced in Fig. 1. All experiments were performed in triplicate and the arithmetic average of the values were used to draw adsorption curves. The amount of dye adsorbed by adsorbents was calculated using Eq. (3):

$$Q_e = \frac{(C_o - C_e) * V}{m} \tag{3}$$

$$\text{Adsorption}\% = \frac{(C_o - C_e)}{C_o} \times 100 \tag{4}$$

where Q_e is the dye adsorption capacity (mg/g), V is the solution volume (L), m is the adsorbent amount (g), C_o and C_e are the initial and equilibrium concentrations of dye (mg/L), respectively.

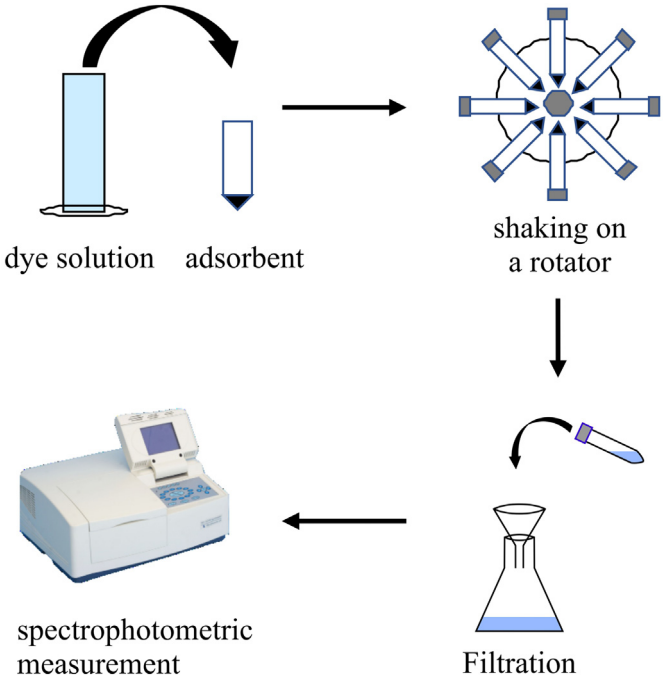

Fig. 1. The schematic diagram of adsorption process.

In addition to R^2 values, Sum of Squared Errors (SSE) values of kinetic results were calculated by the aid of Eq. (5) [27]:

$$SSE = \sum_{n=0}^{n} \left(Q_{e,cal} - Q_{e,\,exp}\right)^2 \tag{5}$$

where $Q_{e,exp}$ is the experimental adsorption capacity at equilibrium, $Q_{e,cal}$ is the calculated adsorption capacity estimated from the kinetic and isotherm models.

2.6. Desorption and reusability of adsorbent

0.05 g sPEEK samples were loaded with 10 mL 200 mg/L dye solutions. Then, the suspensions were centrifuged at 4500 rpm for 5 min, the amount of dyes in centrifugate was determined by spectrophotometric measurement at related wavelength. The dye-loaded sPEEK was washed with 5 mL distilled water, centifugated and decanted. Desorption experiments were carried out by shaking the loaded sorbents with 10 mL of 3 M HNO_3/EtOH (30/70; *v*/v) mixtures at 25 rpm for 20 min, then spectrophotometric measurement of dyes in centrifugate was performed. The desorbed adsorbent was reloaded with 10 mL 200 mg/L dye solution second time. The following desorption steps were performed in the same way as described above. Overall, the adsorption and desorption cycles described above repeated for five times in a continuous manner. The removal efficiency (%) was calculated using Eq. (4) to find the regeneration performance of sPEEK adsorbent.

3. Results and discussion

3.1. Characterization of adsorbent

The FTIR spectra of pure PEEK, sPEEK and dye loaded sPEEK samples are shown in Fig. 2.

The broad band appearing in the FT-IR spectrum of sPEEK with a wavelength of 3400 cm^{-1} was attributed to the O–H vibrations of the sulfonic acid groups formed on the polymer backbone by the sulfonation process. Similarly, the presence of sulfonic acid groups was evidenced by the symmetrical-asymmetrical stretching vibrations (O=S=O) appearing at wavelengths of 1010, 1080 and 1270 cm^{-1} [28,29]. Aromatic C=C stretching band observed at 1596 cm^{-1} wavelength was detected in all samples. The vibration attributed to the

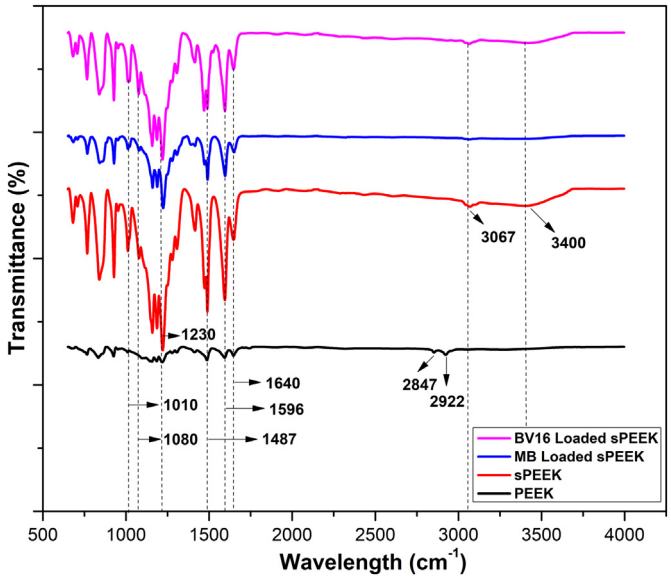

Fig. 2. FTIR spectra of pure PEEK, sPEEK, MB loaded sPEEK and BV16 loaded sPEEK samples.

carbonyl group (C=O) appeared in all samples at a wavelength of 1640 cm^{-1}. The presence of the aromatic (C–C) ring for pure PEEK was evidenced by a single vibration at 1487 cm^{-1} wavelength corresponding to its 1,4-substitution. This peak appeared at two separate vibrations (1463 and 1487 cm^{-1}) for sPEEK. This separation represents the aromatic C–C ring between the two ether bonds. The sulfonic acid groups were attached only to the 1, 2, 4-substituted aromatic ring between the two ether linkages [30]. When the MB loaded sPEEK sample was examined, it was seen that the 3400 cm^{-1} band —which is attributed to the O–H vibrations of the sulfonic acid groups formed by the sulfonation process— was destroyed. This proved that MB adsorption occured by linking the O–H groups. Similarly, the intensity of the OH groups attached to the molecular water present in the sulfonic acid groups decreased in the BV16 loaded sample compared to the sPEEK adsorbent. It was observed that the -OH groups were not completely destroyed in B16 loaded sample, as there was physical immobilization as well as binding to OH groups. Desorption experiments of B16 contaminants also confirm this immobilization and chemical bonding, as well as physical attachment.

The SD of the sPEEK expresses in terms of the number of -SO_3H functional groups per average repeat unit in the polymer backbone. The sulfonation process can also be carried out with sulfonation agents such as oleum or chlorosulfonic acid. However, when this is the case, crosslinking or oligomer formations can be observed [31]. Consequently, the sulfonation process was carried out with 98% sulfuric acid in this study. In the literature, the sulfonation processes performed with different sulfonation agents were carried out at different reaction times and the resulting products with different SD were used for different applications such as fuel cell [32,33], gas separation [34], nanofiltration [35] *etc.* The SD and IEC values of the sPEEK adsorbent used for cationic dyes removal were determined as 0.80 and 2.16 meq/g, respectively.

Further measurements such as BET/N_2 surface area, zeta potential at pH 4.7 and the size distribution interval of 50% of particles ($d_{0.5}$) were determined as 236.3 m^2/g, −29.4 ± 1.7 mV and 290–390 nm, respectively. The surface area of adsorbent is quite high and hence convenient for allowing efficient adsorption. Majority of the natural and synthetic adsorbents have lower surface area than sPEEK adsorbent used in this study [36–39]. High absolute value of zeta potential indicated that sPEEK suspension was stable at pH 4.7 demonstrating and extra benefit for adsorption process. Additionally, it was found that the size of sPEEK particles used in this study were smaller than many adsorbents that have been reported in open literature [40–42]. Given that the reduction in particles size causes more stable suspension [43], it is evident that such small size of sPEEK provides an adventage over other materials in terms of suspension stability and hence adsorption efficiency.

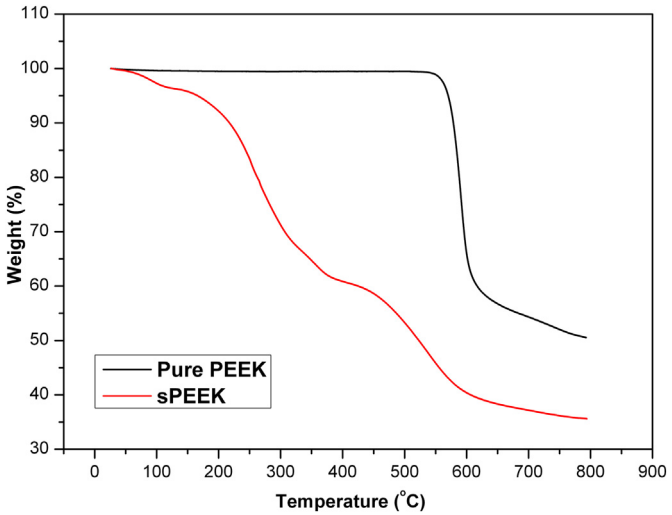

Fig. 3. TGA curves of pure PEEK and sPEEK samples.

One of the most desirable properties of polymeric materials utilizzed in adsorption applications is high thermal stability. In order to investigate the thermal behavior of sPEEK (SD with 0.80) adsorbent used in MB adsorption was performed by TGA. The TGA curves of pure PEEK and sPEEK samples are introduced in Fig. 3.

It is reported in the literature that the initial temperature of weight loss for pure PEEK is about 450–600 °C [44,45]. As seen from the figure, pure PEEK sample showed one step degradation at 550–600 °C, while sPEEK sample had three degradation steps. In pure PEEK polymer matrix, thermal degradation occurred only due to the degradation of the main polymer chain and pure PEEK polymer did not undergo thermal degradation up to 550 °C. As the polymer backbone began to degrade, 50% weight loss was observed at approximately 800 °C. As seen from TGA curve of sPEEK, the first degradation step observed at around 60–130 °C was due to the evaporation of the moisture adsorbed on sPEEK adsorbent. The second thermal decomposition step occured in the temperature range of 150–250 °C was attributed to the degradation of sulfonic acid groups presented in the polymer backbone. The final degradation observed around 450–600 °C is due to the degradation of the polymer main chain [46,47]. These results suggested that sPEEK adsorbent prepared for MB adsorption exhibits sufficient thermal stability considering high-temperature adsorption processes.

The SEM images (with 2500× magnification) of sPEEK and dye loaded sPEEK samples are shown in Fig. 4 a, b, c respectively.

As seen from Fig. 4a, the sPEEK adsorbent has a homogeneous and hollow structure. Light colored structures indicating the filled gaps in the polymer structure were seen in the SEM image of the adsorbent examined after adsorption process (Figs. 4b, c). MB and BV16 deposits were clearly visible, with an open rank in the voids of the pure adsorbent.

3.2. pH effect on dye adsorption

As seen from Fig. 5, the maximum MB and BV16 adsorptions on sPEEK was achieved at pH range between 1 and 3. On the other hand, the adsorption ratio is significantly high below pH 3. The surface of sPEEK carries sulfonic groups (-SO_3H) having highly acidic character [48]. The surface of sPEEK converts from protonated (neutral) form to deprotonated (negatively charged) form beyond pHs between 1 and 3 due to the acidity constant of sPEEK is 1.58 [49]. Partly occured deprotonated form of surface in this pH range may have interacted with the positively charged cationic dyes and may have cause significant adsorption below pH 3. By the way, the significant adsorption at highly acidic pHs (below pH 1) makes think that further interactions such as π-π electron donor-acceptor interactions could be possible. Similar result was obtained rhodamine B adsorption onto sPEEK [49].

3.3. Kinetic evaluations

The decreases in dye concentrations in the suspension over time are shown in Fig. 6a.

As seen from Fig. 6 a, while the equilibrium was attained in 30 min for MB adsorption, the adsorption rate was higher in the first 20 min suggesting rapid occupation of empty active sites due to initially high concentration gradient between surface sites and the bulk solution. Similar situation was observed for BV16 adsorption. The time required for achieving equilibrium was shorter than that of MB adsorption. The pseudo first and second-order, Elovich, Bangham's and intra-particle diffusion kinetic models were applied to determine the kinetic parameters of dyes adsorptions on sPEEK. The results were given in Table 1. Comparision the determination coefficient values (R^2) and Sum of Squared Errors (SSE) values reveals that the pseudo second order kinetic model presents the best agrement with the experimental data. The pseudo second order model indicates that the surface adsorption

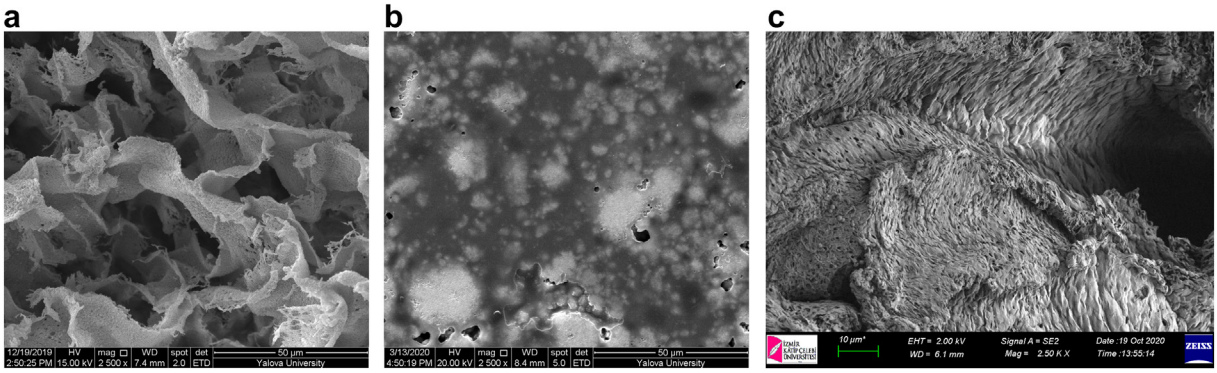

Fig. 4. SEM images of (a) pure sPEEK, (b) MB loaded sPEEK, (c) BV16 loaded sPEEK samples.

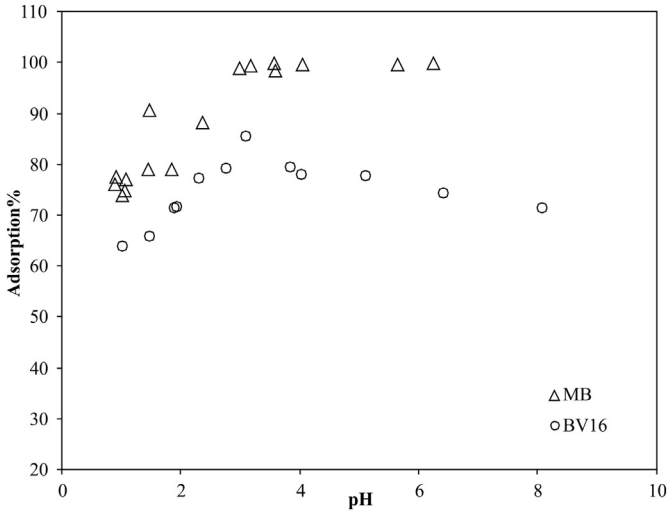

Fig. 5. pH dependency curve for MB and BV16 adsorptions (Solid/liquid = 5 g/L, $T = 298$ K, for MB $C_o = 250$ ppm, $t = 40$ min, for BV16 $C_o = 700$ ppm, $t = 20$ min)

involves chemisorption which is the rate-limiting step, and the migration of sorbate from solution to solid phase is sourced from physicochemical interactions of sorbate with liquid and solid phases [50]. The chemisorption of dyes may be attributed to the interactions between the anionic groups (mainly -SO_3^- groups) of sPEEK and the cationic groups of dyes. The disapperance of the OH band at 3400 cm^{-1} in FTIR spectrum of unloaded sPEEK sample after MB loading supports these interactions. On the other hand, as seen from graph in Fig. 6 b, the Q_t *vs* $t^{1/2}$ graphs have linear regions. The linear regions show that the adsorption involves pore diffusion. However this intraparticle diffusion is not the rate-limiting step (the adsorption processes are not diffusion controlled) because the extrapolation of linear lines do not pass through the origin (Fig. 6b). Relatively low determination coefficient obtained from application of Bangham's Model also supports this explanation [51]. The Elovich (Roginsky–Zeldovich) model explains the chemical adsorption mechanism by taking into account the adsorption rate constant and desorption rate constant. That the initial MB adsorption rate constant onto sPEEK is approximately one hundred times greater than desorption rate constant, and rather high initial adsorption rate of BV16 (as seen from Fig. 6a) point out the high adsorption affinity of cationic dyes on sPEEK.

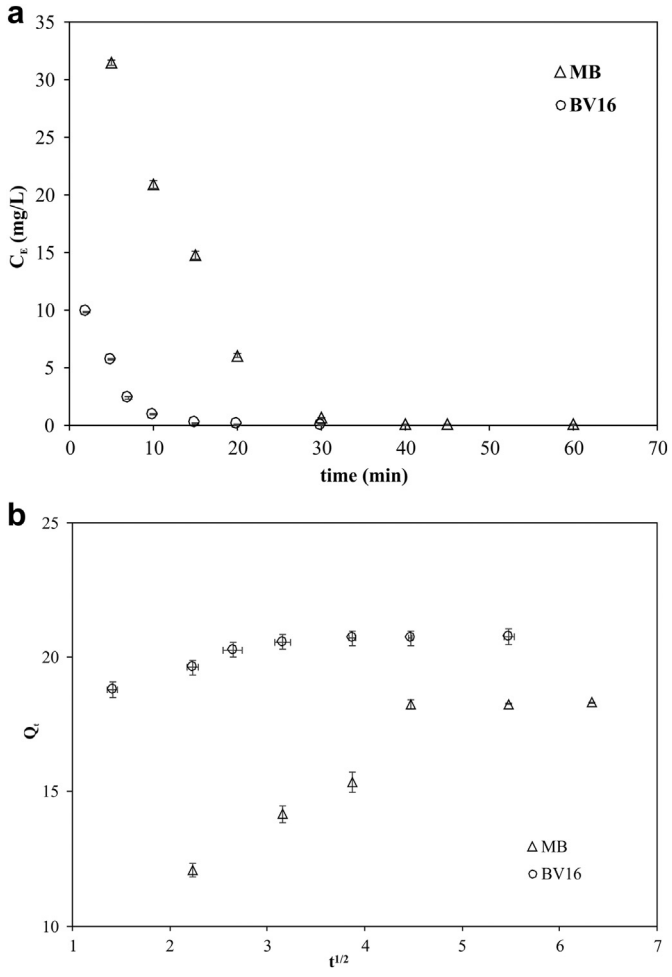

Fig. 6. a) Time dependent decreasing of equilibrium concentrations of dyes, b) the curve of intraparticle diffusion kinetic model (Solid/liquid = 5 g/L, $C_o = 100$ mg/L, $T = 298$ K, pH = 3.5 for MB, pH = 2.7 for BV16).

3.4. Adsorption isotherm

Fig. 7 shows adsorbed amount of dyes on adsorbents depending the initial concentration of dye solutions. As observed from the figure, sulfonation of PEEK enhanced the adsorption of methylene blue. The maximum MB adsorption capacity (in mmol/g) of sPEEK is six times higher than the capacity of PEEK.

The PEEK does not have any functional groups having affinity for cationic dyes. On the other hand, low adsorption can be explained by

Table 1
Kinetic results of dye adsorptions obtained from linearized models.

	k_1 1/min	k_2 g/mg min	$Q_{E\ cal.}$, mg/g	k_i mg $min^{1/2}$/g	k_0 L/(mg/L)	$\alpha_{Banghams}$	$\alpha_{Elovich}$ mg/g min	β g/mg	R^2	SSE
MB Adsorption										
Pseudo-first order model	0.14		15.50						0.992	250.4
$Log\ (Q_E\text{-}Q_t) = Log\ Q_E - (k_1/2.303)\ t$[a]										
Pseudo-second order model		0.01	20.41						0.998	174.9
$t/Q_t = 1/k_2 Q_E^2 + (1/Q_E)\ t$[a]										
Intraparticle diffusion model				1.88					0.997	26.3
$Q_t = k_i t^{1/2} + C$[a]										
Bangham's model					3.6×10^{-4}	1.9			0.875	4×10^4
$Log\ [C_0/(C_0 - Q_t\ m)] = Log\ [(k_0\ m)/(2.303\ V)] + \alpha\ Log\ t$[a]										
Elovich Model							28.25	0.31	0.984	7.1×10^4
$Q_t = (1/\beta)\ ln(\alpha\ \beta) + (1/\beta)\ ln\ t$[a]										
BV16 Adsorption										
Pseudo-first order model	0.23		2.64						0.935	1803.8
Pseudo-second order model		0.2	20.9						1.000	6.96
Intraparticle diffusion model				0.81					0.911	0.9
Bangham's model					7×10^{-3}	1.9			0.935	5×10^4
Elovich Model							2.6×10^{10}	1.31	0.884	7.1×10^2

[a] Where k_1 and k_2 are first order rate and second order rate constant, respectively. t is the contact time (min), Q_E is the adsorbed amount of dye at equilibrium, Q_t is the adsorbed amount of dye at any time, k_i is the intraparticle diffusion rate constant, C is the intercept, C_0 is the initial concentration of metal cation (mol/L), V is the volume of solution (mL), m is the solid/liquid ratio (g/L), k_0 and α are the constants, α is the initial adsorption rate (mg/(g min)) and β is the desorption constant (g/mg).

further interactions such as π-π electron donor-acceptor interactions. Alinezdah et al. achieved 70.02 mg/g by using polymeric magnetic boehmite nanocomposite [52], Sahu et al. retained 124.5 mg/g MB on modified lychee seed biochar [53], and Mantasha et al. obtained 98.83 mg/g MB adsorption capacity on Cu(II) based metal organic framework [54]. Many materials having similar or lower adsorption capacity for MB exists in the literature. [55–57]. On the other hand, the maximum adsorption capacity of sPEEK for BV16 was calculated as 181.8 mg/g 0.5 mmol/g. This value is reasonable compared to the limited number of studies in the literature on BV16 removal by adsorption process [18–22]. There are certain studies obtaining higher adsorption capacity both MB and BV16 in literature [9,14,20,23], but all these studies were performed by using adsorbents which were expensively produced and having higher surface area such as magnetite graphene oxide nanocomposites, activated, charred or carbonized materials.

Langmuir, Freundlich, Temkin and Dubinin-Radushkevich (D-R) models were used to analyze adsorption isotherms. The adsorption parameters obtained from the linearized models were given in Table 2.

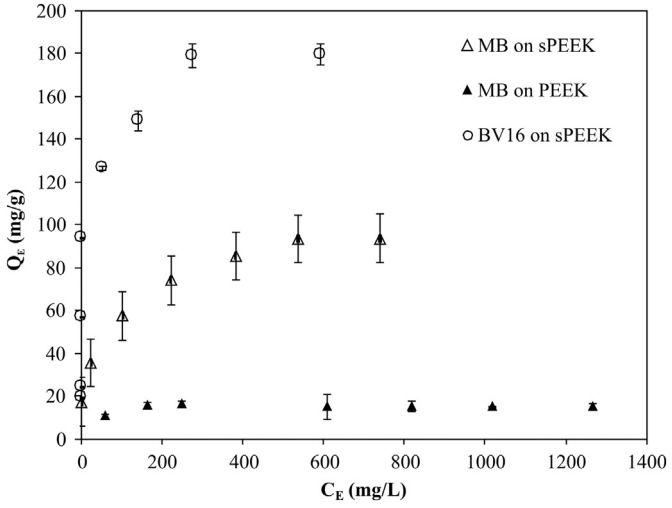

Fig. 7. Isotherm curves of MB and BV16 adsorptions (Solid/liquid = 5 g/L, T = 298 K, pH = 3.5, t = 40 min for MB, pH = 2.7, t = 20 min for BV16).

The dye adsorptions demonstrate Langmuirian character, and this deduction has been supported by Q_E *vs.* C_E graph (Fig. 7).

Taking into account all those results, easy processability of cost-effective adsorbent comparing with carbon based and/or polymeric magnetic nanocomposite, sPEEK can serve as an effective adsorbent for cationic dye removal.

Table 2
Isotherm parameters, calculated from linearized equations, of dye adsorptions.

Linearized Models	Parameters	MB (on sPEEK)	MB (on PEEK)	BV16 (on sPEEK)
Langmuir Isotherm	Q_{max}	98.04	15.24	181.8
$C_E/Q_E = 1/(K_1.Q_{max}) +$	K_L	2.26	9.2	22.7
$(1/Q_{max}).\ C_E$[a]	R^2	0.991	0.999	0.997
	SSE	511.4	18.9	1580.3
Freundlich Isotherm	K_F	25.18	9.12	54.6
$Log\ Q_E = Log\ K_F +$	n	5.15	12.53	4.94
$1/n\ Log\ C_E$[a]	R^2	0.959	0.394	0.723
	SSE	7.8×10^3	6776.3	465
Dubinin- Redushkevich	Q_{max}	69.6	15.7	164.4
Isotherm	β	4×10^{-8}	2×10^{-4}	8×10^{-8}
$Ln\ Q_E = Ln\ Q_{max} - \beta\varepsilon^2$[a]	ε	3.53	50	2500
	R^2	0.702	0.913	0.808
	SSE	2.7×10^3	2.65	2.8×10^3
Temkin Isotherm	B[a]	286.5	2473.1	149.4
$Q_E = (RT/b)\ (Ln\ K_T)$	K_T	28.06	6668.1	81.4
$+ (RT/b)\ (Ln\ C_E)$[a]	R^2	0.847	0.361	0.881
	SSE	814.3	43.2	374

[a] Where Q_e is the amount of dye adsorbed at equilibrium (mg/g), C_e is the equilibrium dye concentration in the solution (mg/L), Q_{max} is the maximum monolayer capacity of the adsorbent (mg/g) and K_L is the Langmuir adsorption constant (L/mg), K_F is Freundlich constant related to adsorption capacity (L/g) and 1/n is the adsorption strength, β is the constant about mean free energy of the adsorption ($mmol^2/kJ^2$), ε (=RTLn(1 + (1/C_E)) is Polanyi potential (J/mmol), RT/b = B is the heat of adsorption (joule/mol) and K_T is Temkin constant related to adsorption capacity (L/mol).

Table 3
The thermodynamic parameters for MB adsorption.

	ΔH° (kJ/mol)	ΔG° (kJ/mol)	ΔS° (J/mol K)
298 K	38.51	−13.38	174
313 K		−15.83	173

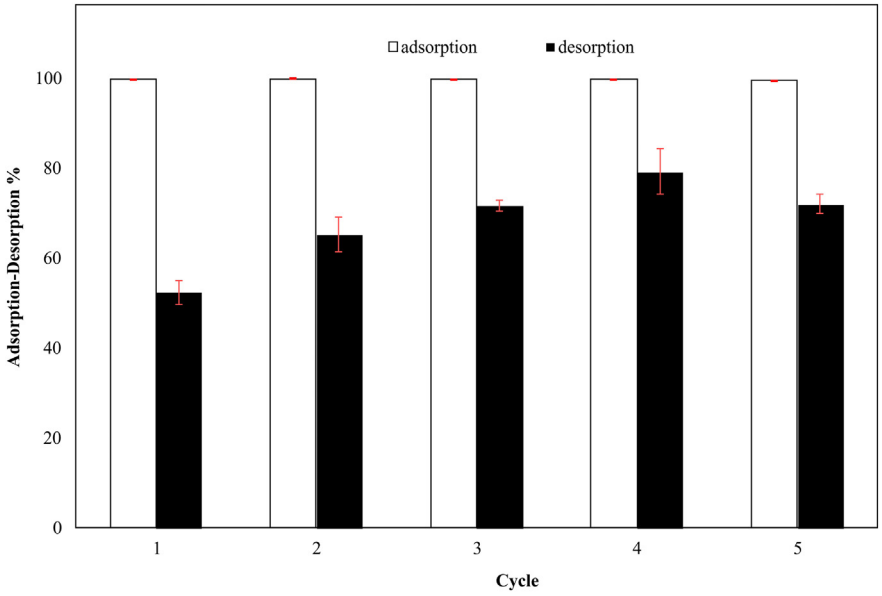

Fig. 8. The adsorption efficiency of MB loaded sPEEK adsorbent after multiple adsorption/desorption cycles (Solid/liquid = 5 g/L, leach solution contact time = 20 min, $T = 298$ K).

3.5. MB Adsorption thermodynamics

The thermodynamic parameters of MB adsorbed on sPEEK were evaluated on the basis of Gibbs free energy change (ΔG^o), entropy change (ΔS^o) and enthalpy change (ΔH^o). The thermodynamic equations are given below (Eqs. 6, 7, 8):

$$\Delta G^o = -RT\ln K_c \tag{6}$$

$$\mathrm{Ln}\frac{k_2}{k_1} = -\frac{\Delta H^o}{R} - \left(\frac{1}{T_2} - \frac{1}{T_1}\right) \tag{7}$$

$$\Delta G^o = \Delta H^o - T\Delta S^o \tag{8}$$

where R (8.314 J/mol K) is the gas constant, T (K) is the temperature, k_1 and k_2 are the Langmuir constant for each temperature and K_C (L/g) is the adsorption equilibrium constant for each temperature which is obtained from Langmuir constants Q_{max} and K_L ($K_C = Q_{max} \times K_L$) [58].

The thermodynamic values calculated from experimental results were tabulated in Table 3.

The MB adsorption onto sPEEK is an endothermic reaction, and spontaneously occurs at 298 K and 313 K. Considering that the magnitude of ΔH° value for chemisorption processes is higher than 20 kJ/mol [59], the enthalpy of MB adsorption reflects chemisorption. The increase in absolute ΔG^o value with increasing temperature shows that the MB adsorption is more favorable at high temperatures. On the other hand, positive value of entrophy change suggests that the randomness on solid/solution interface increases as a result of adsorption.

3.6. Desorption studies

The recovery and reusability of adsorbent material is an important parameter related to the application potential of adsorption technology. Desorption and recycling experiments were conducted to evaluate the reusability of the sPEEK. The results were shown in Fig. 8.

The adsorption efficiency of MB onto sPEEK decreases from 99.6% to 99.2% after five cycles. As seen from Fig. 8, there is a quite small decrease in adsorption efficiencies during multiple adsorption/desorption cycles. These results provides evidence for superior performance of sPEEK and therefore it can be said that sPEEK is very effective reusable adsorbent for MB adsorption.

On the other hand, when BV16 loaded adsorbent was contact with 3 M HNO_3/EtOH (30/70; *v*/v) leaching solution at the same conditions with MB desorption, at least 10% of BV16 was desorbed. The rather high ratio of initial adsorption rate (α) to desorption constant (β) supports this finding.

4. Conclusion

The sPEEK polymeric material was used as adsorbent for cationic dye adsorption in this study, and it was decided that sPEEK is a good adsorbent for MB removal in terms of short contact time, 100 times higher initial adsorption rate than desorption rate and a slight decrease in adsorption efficiency after multiple adsorption/desorption cycles, and decided that sPEEK is an efficient adsorbent to immobilize BV16 with the high adsorption in such a short time as 20 min. The dye adsorptions showed Langmuirian character, and the maximum reached adsorption capacity was 0.29 mmol/g for MB adsorption, and 0.50 mmol/g BV16 adsorption. The kinetic of adsorptions is fitted Pseudo Second-Order Model. Intraparticle diffusion was involved in adsorption, but it was not the rate-limiting step. The maximum dye adsorptions on sPEEK were achieved at pH range between 1 and 3. The physicochemical adsorption of cationic dyes is attributed to the interactions between negatively charged -SO_3^- groups of sPEEK and positively charged dye. Additionally, π-π electron donor-acceptor interactions could be possible. Thermodinamically, MB adsorption is endothermic reaction, and spontaneously occurs at room temperature and above. Moreover, it was showed that the adsorption is more favorable at high temperatures. In conclusion, the results of this study suggests that sPEEK can be a very effective and reusable alternative to conventional adsorbents for cationic dye removal for use in environmental applications.

CRediT authorship contribution statement

Jülide Hızal: Visualization, Writing - original draft, Conceptualization, Writing - review & editing. **Nergiz Kanmaz:** Investigation. **Mesut Yılmazoğlu:** Formal analysis, Investigation.

Declaration of Competing Interest

The authors declare that they have no known competing financial interests or personal relationships that could have appeared to influence the work reported in this paper.

Acknowledgements

The authors would like to thank to Central Laboratory of Yalova University for allowing the use of laboratory facilities while conducting this research.

References

[1] S.T. Ambrósio, G.M. Campos-Takaki, Decolorization of reactive azo dyes by Cunninghamella elegans UCP 542 under co-metabolic conditions, Bioresour. Technol. 91 (2004) 69–75, https://doi.org/10.1016/S0960-8524(03)00153-6.
[2] Z. Wang, M. Gao, X. Li, J. Ning, Z. Zhou, G. Li, Efficient adsorption of methylene blue from aqueous solution by graphene oxide modified persimmon tannins, Mater. Sci. Eng. C 108 (2020) 110196, https://doi.org/10.1016/j.msec.2019.110196.
[3] J.Y. Yang, X.Y. Jiang, F.P. Jiao, J.G. Yu, The oxygen-rich pentaerythritol modified multi-walled carbon nanotube as an efficient adsorbent for aqueous removal of alizarin yellow R and alizarin red S, Appl. Surf. Sci. 436 (2018) 198–206, https://doi.org/10.1016/j.apsusc.2017.12.029.
[4] R.R. Ramsay, C. Dunford, P.K. Gillman, Methylene blue and serotonin toxicity: inhibition of monoamine oxidase a (MAO a) confirms a theoretical prediction, Br. J. Pharmacol. 152 (2007) 946–951, https://doi.org/10.1038/sj.bjp.0707430.
[5] F. Temel, M. Turkyilmaz, S. Kucukcongar, Removal of methylene blue from aqueous solutions by silica gel supported calix[4]arene cage: investigation of adsorption properties, Eur. Polym. J. 125 (2020) 109540, https://doi.org/10.1016/j.eurpolymj.2020.109540.
[6] A.K. Verma, R.R. Dash, P. Bhunia, A review on chemical coagulation/flocculation technologies for removal of colour from textile wastewaters, J. Environ. Manag. 93 (2012) 154–168, https://doi.org/10.1016/j.jenvman.2011.09.012.
[7] X.C. Ruan, M.Y. Liu, Q.F. Zeng, Y.H. Ding, Degradation and decolorization of reactive red X-3B aqueous solution by ozone integrated with internal micro-electrolysis, Sep. Purif. Technol. 74 (2010) 195–201, https://doi.org/10.1016/j.seppur.2010.06.005.
[8] S. Varnagiris, M. Urbonavicius, S. Sakalauskaite, R. Daugelavicius, L. Pranevicius, M. Lelis, D. Milcius, Floating TiO2 photocatalyst for efficient inactivation of *E. coli* and decomposition of methylene blue solution, Sci. Total Environ. 720 (2020)https://doi.org/10.1016/j.scitotenv.2020.137600.
[9] X. Jiang, H. Xia, L. Zhang, S. Cheng, Q. Zhang, Q. Chen, W. Hu, Synthesis of copper-loaded activated carbon for enhancing the photocatalytic removal of methylene blue, J. Mol. Liq. 272 (2018) 353–360, https://doi.org/10.1016/j.molliq.2018.09.087.
[10] M.M. El-Moselhy, S.M. Kamal, Selective removal and preconcentration of methylene blue from polluted water using cation exchange polymeric material, Groundw. Sustain. Dev. 6 (2018) 6–13, https://doi.org/10.1016/j.gsd.2017.10.001.
[11] F. Gut, W. Schiek, W.E. Haefeli, I. Walter-Sack, J. Burhenne, Cation exchange resins as pharmaceutical carriers for methylene blue: binding and release, Eur. J. Pharm. Biopharm. 69 (2008) 582–587, https://doi.org/10.1016/j.ejpb.2007.12.016.
[12] Y. Liu, Y. Zheng, A. Wang, Enhanced adsorption of methylene blue from aqueous solution by chitosan-g-poly (acrylic acid)/vermiculite hydrogel composites, J. Environ. Sci. 22 (2010) 486–493, https://doi.org/10.1016/S1001-0742(09)60134-0.
[13] H. Deng, J. Lu, G. Li, G. Zhang, X. Wang, Adsorption of methylene blue on adsorbent materials produced from cotton stalk, Chem. Eng. J. 172 (2011) 326–334, https://doi.org/10.1016/j.cej.2011.06.013.
[14] Y. Wang, Z. Wang, S. Wang, Z. Chen, J. Chen, Y. Chen, J. Fu, Magnetic poly (cyclotriphosphazene-co-4,4′-sulfonyldiphenol) nanotubes modified with glacial acetic acid for removing methylene blue: adsorption performance and mechanism, Eur. Polym. J. 120 (2019) 109198, https://doi.org/10.1016/j.eurpolymj.2019.08.025.
[15] A.A.A. Darwish, M. Rashad, H.A. AL-Aoh, Methyl orange adsorption comparison on nanoparticles: isotherm, kinetics, and thermodynamic studies, Dyes Pigments 160 (2019) 563–571, https://doi.org/10.1016/j.dyepig.2018.08.045.
[16] Ş. Yılmaz, A. Zengin, Ü. Ecer, T. Şahan, Conversion from a natural mineral to a novel effective adsorbent: utilization of pumice grafted with polymer brush for methylene blue decolorization from aqueous environments, Colloids Surfaces A Physicochem. Eng. Asp. 583 (2019)https://doi.org/10.1016/j.colsurfa.2019.123961.
[17] A.K. Prajapati, M.K. Mondal, Comprehensive kinetic and mass transfer modeling for methylene blue dye adsorption onto CuO nanoparticles loaded on nanoporous activated carbon prepared from waste coconut shell, J. Mol. Liq. 307 (2020) 112949, https://doi.org/10.1016/j.molliq.2020.112949.
[18] S. Afshin, Y. Rashtbari, M. Shirmardi, M. Vosoughi, A. Hamzehzadeh, Adsorption of basic violet 16 dye from aqueous solution onto mucilaginous seeds of Salvia sclarea: kinetics and isotherms studies, Desal. Water Treat. 161 (2019) 365–375, https://doi.org/10.5004/dwt.2019.24265.
[19] Z. Rahmani, M. Kermani, M. Gholami, A.J. Jafari, N.M. Mahmoodi, Effectiveness of photochemical and sonochemical processes in degradation of basic violet 16 (BV16) dye from aqueous solutions, Iran. J. Environ. Health Sci. Eng. 9 (2012) 14, https://doi.org/10.1186/1735-2746-9-14.
[20] E.K. Shirazi, J.W. Metzger, K. Fischer, A.H. Hassani, Removal of textile dyes from single and binary component systems by Persian bentonite and a mixed adsorbent of bentonite/charred dolomite, Colloids Surf. A Physicochem. Eng. Asp. 598 (2020) 124807, https://doi.org/10.1016/j.colsurfa.2020.124807.
[21] N.M. Mahmoodi, M. Arami, H. Bahrami, S. Khorramfar, Novel biosorbent (*Canola* hull): surface characterization and dye removal ability at different cationic dye concentrations, Desalination 264 (1–2) (2010) 134–142, https://doi.org/10.1016/j.desal.2010.07.017.
[22] M.P.E. González, J. Mattusch, A.A.P. Cid, R. Wennrich, Characterization of adsorbent materials prepared from avocado kernel seeds: natural, activated and carbonized forms, J. Anal. Appl. Pyrolysis 78 (1) (2007) 185–193, https://doi.org/10.1016/j.jaap.2006.06.008.
[23] M. Alipour, M. Vosoughi, S.A. Mokhtari, H. Sadeghi, Y. Rashtbari, M. Shirmardi, R. Azad, Optimising the basic violet 16 adsorption from aqueous solutions by magnetic graphene oxide using the response surface model based on the Box–Behnken design, Int. J. Environ. Anal. Chem. (2019)https://doi.org/10.1080/03067319.2019.1671378.
[24] F. Mehri, M. Ghamati, S. Rowshanzamir, W. Sauter, U. Schröder, Evaluation of the membrane efficiency of both Nafion and sulfonated poly (ether ether ketone) using electrochemical membrane reactor toward desulfurization of a model diesel fuel, Chem. Eng. Res. Des. 153 (2020) 517–527, https://doi.org/10.1016/j.cherd.2019.11.007.
[25] M.M. Nasef, A.H. Yahaya, Adsorption of some heavy metal ions from aqueous solutions on Nafion 117 membrane, Desalination 249 (2009) 677–681, https://doi.org/10.1016/j.desal.2008.12.059.
[26] W.Y. Wang, Y. Ku, Effect of solution pH on the adsorption and photocatalytic reaction behaviors of dyes using TiO2 and Nafion-coated TiO2, Colloids Surfaces A Physicochem. Eng. Asp. 302 (2007) 261–268, https://doi.org/10.1016/j.colsurfa.2007.02.037.
[27] A.M. Elgarahy, K.Z. Elwakeel, G.A. Elshoubaky, S.H. Mohammad, Microwave-accelerated sorption of cationic dyes onto green marine algal biomass, Environ. Sci. Pollut. Res. 26 (2019) 22704–22722, https://doi.org/10.1007/s11356-019-05417-2.
[28] J.M. Song, J. Shin, J.Y. Sohn, Y.C. Nho, Preparation and characterization of SPEEK membranes crosslinked by electron beam irradiation, Macromol. Res. 19 (2011) 1082–1089, https://doi.org/10.1007/s13233-011-1013-7.
[29] P. Xing, G.P. Robertson, M.D. Guiver, S.D. Mikhailenko, K. Wang, S. Kaliaguine, Synthesis and characterization of sulfonated poly(ether ether ketone) for proton exchange membranes, J. Membr. Sci. 229 (2004) 95–106, https://doi.org/10.1016/j.memsci.2003.09.019.
[30] E. Drioli, A. Regina, M. Casciola, A. Oliveti, F. Trotta, T. Massari, Sulfonated PEEK-WC membranes for possible fuel cell applications, J. Membr. Sci. 228 (2004) 139–148, https://doi.org/10.1016/j.memsci.2003.07.023.
[31] L. Li, J. Zhang, Y. Wang, Sulfonated poly(ether ether ketone) membranes for direct methanol fuel cell, J. Membr. Sci. 226 (2003) 159–167, https://doi.org/10.1016/j.memsci.2003.08.018.
[32] J. Jaafar, A.F. Ismail, T. Matsuura, K. Nagai, Performance of SPEEK based polymer-nanoclay inorganic membrane for DMFC, J. Membr. Sci. 382 (2011) 202–211, https://doi.org/10.1016/j.memsci.2011.08.016.
[33] Şengül Erce, H. Erdener, R.G. Akay, H. Yücel, N. Baç, I.I. Eroğlu, Effects of sulfonated polyether-etherketone (SPEEK) and composite membranes on the proton exchange membrane fuel cell (PEMFC) performance, Int. J. Hydrog. Energy 34 (2009) 4645–4652, https://doi.org/10.1016/j.ijhydene.2008.08.066.
[34] A.L. Khan, X. Li, I.F.J. Vankelecom, SPEEK/Matrimid blend membranes for CO2 separation, J. Membr. Sci. 380 (2011) 55–62, https://doi.org/10.1016/j.memsci.2011.06.030.
[35] W.J. Lau, A.F. Ismail, Effect of SPEEK content on the morphological and electrical properties of PES/SPEEK blend nanofiltration membranes, Desalination 249 (2009) 996–1005, https://doi.org/10.1016/j.desal.2009.09.016.
[36] O. Kazak, Y.R. Eker, H. Bingol, A. Tor, Preparation of chemically-activated high surface area carbon from waste vinasse and its efficiency as adsorbent material, J. Mol. Liq. 272 (2018) 189–197, https://doi.org/10.1016/j.molliq.2018.09.085.
[37] P. Rodríguez-Estupiñán, M.S. Legnoverde, S. Simonetti, A. Díaz Compañy, A. Juan, L. Giraldo, J.C. Moreno-Piraján, E.I. Basaldella, Influence of functionalization, surface area and charge distribution of SBA15-based adsorbents on CO (II) and NI (II) removal from aqueous solutions, J. Environ. Chem. Eng. 8 (2020) 103671, https://doi.org/10.1016/j.jece.2020.103671.
[38] F. Ma, Y. Gui, P. Liu, Y. Xue, W. Song, Functional fibrous materials-based adsorbents for uranium adsorption and environmental remediation, Chem. Eng. J. 390 (2020) 124597, https://doi.org/10.1016/j.cej.2020.124597.
[39] A. Flilissa, S. Venkataraman, K. Laouameur, A. Beroual, O. Flilissa, K. Omine, T. Chaabane, A. Darchen, Surface modification of aluminum phosphate by sodium dodecylbenzenesulfonate (SDBS): a new nano-structured adsorbent for an improved removal of Ponceau S, J. Environ. Chem. Eng. 8 (2020)https://doi.org/10.1016/j.jece.2019.103625.
[40] S. Kara, C. Aydiner, E. Demirbas, M. Kobya, N. Dizge, Modeling the effects of adsorbent dose and particle size on the adsorption of reactive textile dyes by fly ash, Desalination 212 (2007) 282–293, https://doi.org/10.1016/j.desal.2006.09.022.
[41] P. Mondal, C.B. Majumder, B. Mohanty, Effects of adsorbent dose, its particle size and initial arsenic concentration on the removal of arsenic, iron and manganese from simulated ground water by Fe3+ impregnated activated carbon, J. Hazard. Mater. 150 (2008) 695–702, https://doi.org/10.1016/j.jhazmat.2007.05.040.
[42] S. Mun, Enhanced performance of a tandem simulated moving bed process for separation of paclitaxel, 13-dehydroxybaccatin III, and 10-deacetylpaclitaxel by making a difference between the adsorbent particle sizes of the two subordinate simulated moving bed units, Process Biochem. 46 (2011) 1329–1334, https://doi.org/10.1016/j.procbio.2011.02.026.

[43] D. Zhu, Y. Shen, L. Wei, L. Xu, X. Cao, H. Liu, J. Li, Effect of particle size on the stability and flavor of cloudy apple juice, Food Chem. 328 (2020)https://doi.org/10.1016/j.foodchem.2020.126967.
[44] P. Knauth, H. Hou, E. Bloch, E. Sgreccia, M.L. Di Vona, Thermogravimetric analysis of SPEEK membranes: thermal stability, degree of sulfonation and cross-linking reaction, J. Anal. Appl. Pyrolysis 92 (2011) 361–365, https://doi.org/10.1016/j.jaap.2011.07.012.
[45] G.M. Shashidhara, K.N. Kumar, Proton conductivity of SPEEK membranes, Polym.-Plast. Technol. Eng. 49 (2010) 796–806, https://doi.org/10.1080/03602551003749601.
[46] D.J. Kim, D.H. Choi, C.H. Park, S.Y. Nam, Characterization of the sulfonated PEEK/sulfonated nanoparticles composite membrane for the fuel cell application, Int. J. Hydrog. Energy 41 (2016) 5793–5802, https://doi.org/10.1016/j.ijhydene.2016.02.056.
[47] S. Yi, F. Zhang, W. Li, C. Huang, H. Zhang, M. Pan, Anhydrous elevated-temperature polymer electrolyte membranes based on ionic liquids, J. Membr. Sci. 366 (2011) 349–355, https://doi.org/10.1016/j.memsci.2010.10.031.
[48] M.S. Gruzdev, L.E. Shmukler, N.O. Kudryakova, A.M. Kolker, Y.A. Sergeeva, L.P. Safonova, Triethanolamine-based protic ionic liquids with various sulfonic acids: synthesis and properties, J. Mol. Liq. 242 (2017) 838–844, https://doi.org/10.1016/j.molliq.2017.07.078.
[49] N. Kanmaz, M. Acar, M. Yılmazoğlu, J. Hızal, Rhodamine B and murexide retention onto sulfonated poly (ether ether ketone) (sPEEK), Colloids Surf. A Physicochem. Eng. Asp. 605 (2020) 125341, https://doi.org/10.1016/j.colsurfa.2020.125341.
[50] H. Wang, A. Zhou, F. Peng, H. Yu, J. Yang, Mechanism study on adsorption of acidified multiwalled carbon nanotubes to Pb(II), J. Colloid Interface Sci. 316 (2007) 277–283, https://doi.org/10.1016/j.jcis.2007.07.075.
[51] M. Yilmazoglu, J. Hizal, Chapter 7: Kinetic evaluation of heavy metals and organic pollutions adsorption on clays, Engineering Research Papers, Gece Akademi 2019, pp. 117–141.
[52] H. Alinezhad, M. Zabihi, D. Kahfroushan, Design and fabrication the novel polymeric magnetic boehmite nanocomposite (boehmite@ Fe3O4@PLA@SiO2) for the remarkable competitive adsorption of methylene blue and mercury ions, J. Phys. Chem. Solids 144 (2020) 109515, https://doi.org/10.1016/j.jpcs.2020.109515.
[53] S. Sahu, S. Pahi, S. Tripathy, S.K. Singh, A. Behera, U.K. Sahu, R.K. Patel, Adsorption of methylene blue on chemically modified lychee seed biochar: dynamic, equilibrium, and thermodynamic study, J. Mol. Liq. 315 (2020) 113743, https://doi.org/10.1016/j.molliq.2020.113743.
[54] I. Mantasha, H.A.M. Saleh, K.M.A. Qasem, M. Shahid, M. Mehtab, M. Ahmad, Efficient and selective adsorption and separation of methylene blue (MB) from mixture of dyes in aqueous environment employing a Cu(II) based metal organic framework, Inorg. Chim. Acta 511 (2020) 119787, https://doi.org/10.1016/j.ica.2020.119787.
[55] Y. Zhang, J. Liu, X. Du, W. Shao, Preparation of reusable glass hollow fiber membranes and methylene blue adsorption, J. Eur. Ceram. Soc. 39 (2019) 4891–4900, https://doi.org/10.1016/j.jeurceramsoc.2019.06.038.
[56] F.M. Mpatani, A.A. Aryee, A.N. Kani, Q. Guo, E. Dovi, L. Qu, Z. Li, R. Han, Uptake of micropollutant-bisphenol A, methylene blue and neutral red onto a novel bagasse-β-cyclodextrin polymer by adsorption process, Chemosphere 259 (2020) 127439, https://doi.org/10.1016/j.chemosphere.2020.127439.
[57] S. Soni, P.K. Bajpai, J. Mittal, C. Arora, Utilisation of cobalt doped Iron based MOF for enhanced removal and recovery of methylene blue dye from waste water, J. Mol. Liq. 314 (2020) 113642, https://doi.org/10.1016/j.molliq.2020.113642.
[58] H. Karaer, I. Kaya, Synthesis, characterization of magnetic chitosan/active charcoal composite and using at the adsorption of methylene blue and reactive blue4, Microporous Mesoporous Mater. 232 (2016) 26–38, https://doi.org/10.1016/j.micromeso.2016.06.006.
[59] R. Khamirchi, A. Hosseini-Bandegharaei, A. Alahabadi, S. Sivamani, A. Rahmani-Sani, T. Shahryari, I. Anastopoulos, M. Miri, H.N. Tran, Adsorption property of Br-PADAP-impregnated multiwall carbon nanotubes towards uranium and its performance in the selective separation and determination of uranium in different environmental samples, Ecotoxicol. Environ. Saf. 150 (2018) 136–143, https://doi.org/10.1016/j.ecoenv.2017.12.039.